Inorg. Chem. **1981**, *20*, 3823–3828

Contribution from the Departments of Chemistry, Brookhaven National Laboratory, Upton, New York 11973,
The Pennsylvania State University, University Park, Pennsylvania 16802, and the
University of Southern California, Los Angeles, California 90007

Preparation and Structural Characterization of $[(Ph_3P)_2N][HFeRu_3(CO)_{13}]$ and $[(Ph_3P)_2N][HFe_2Ru_2(CO)_{13}]$

F. TAKUSAGAWA,[1a] A. FUMAGALLI,[1a,d] T. F. KOETZLE,*[1a] G. R. STEINMETZ,[1b] R. P. ROSEN,[1b] W. L. GLADFELTER,[1b] G. L. GEOFFROY,*[1b] M. A. BRUCK,[1c] and R. BAU*[1c]

Received January 27, 1981

Reaction of $[(Ph_3P)_2N][HFe(CO)_4]$ with $Ru_3(CO)_{12}$ and $Fe_2Ru(CO)_{12}$ in refluxing THF gives the new clusters $[(Ph_3P)_2N][HFeRu_3(CO)_{13}]$ and $[(Ph_3P)_2N][HFe_2Ru_2(CO)_{13}]$ in 47% and 4% yields, respectively. $[(Ph_3P)_2N][HFeRu_3(CO)_{13}]$ has been characterized by its spectroscopic properties and by complete single-crystal X-ray and neutron diffraction studies. $[(Ph_3P)_2N][HFeRu_3(CO)_{13}]$ crystallizes in the space group $P\bar{1}$ with $Z = 2$. Unit cell dimensions from the neutron diffraction study at 15 K are $a = 15.053$ (2) Å, $b = 9.073$ (1) Å, $c = 18.992$ (3) Å, $\alpha = 104.75$ (2)°, $\beta = 109.58$ (2)°, and $\gamma = 86.95$ (2)°. The structure was refined to $R(F^2) = 0.052$ and $R(wF^2) = 0.057$ with measured intensities of 8354 independent reflections. The $[HFeRu_3(CO)_{13}]^-$ anion has a closed pseudotetrahedral structure with each Ru bearing three terminal carbonyls. Two terminal carbonyls are attached to Fe with two additional carbonyls occupying semibridging positions between Fe and two Ru atoms. The hydride ligand symmetrically bridges one of the Ru–Ru bonds. $[(Ph_3P)_2N][HFe_2Ru_2(CO)_{13}]$ has also been characterized crystallographically. It crystallizes in the space group $P\bar{1}$ with $Z = 2$. The unit cell dimensions at room temperature are $a = 14.955$ (2) Å, $b = 18.144$ (3) Å, $c = 9.290$ (2) Å, $\alpha = 101.54$ (2)°, $\beta = 95.03$ (4)°, and $\gamma = 84.04$ (3)°. The structure was solved and refined to $R(F) = 0.056$ and $R(wF) = 0.042$ for 5886 independent reflections with $I \geq 3.0\sigma(I)$. The structure of $[HFe_2Ru_2(CO)_{13}]^-$ is similar to that of $[HFeRu_3(CO)_{13}]^-$ except that the anion possesses a full-bridging CO between the two Fe atoms and no semibridging CO's.

The $[H_xM_4(CO)_{13}]^{(2-x)-}$ series of clusters (M = Fe and/or Ru) exists in an interesting variety of structural forms. The neutral clusters $H_2Ru_4(CO)_{13}$[2] and $H_2FeRu_3(CO)_{13}$[3] have closed pseudotetrahedral geometries, each with two long Ru–Ru bonds that are believed to correspond to Ru–H–Ru bridges. The deprotonated cluster $[Fe_4(CO)_{13}]^{2-}$[4] contains a triply bridging (face-bridging) carbonyl group which is not present in $H_2Ru_4(CO)_{13}$ or $H_2FeRu_3(CO)_{13}$. In contrast, the geometry of $[HFe_4(CO)_{13}]^-$[5] is radically different from the others: it possesses an "open-butterfly" arrangement of metal atoms, with a unique four-electron carbonyl group bound in a σ–π ("sideways") fashion.

Because of the relevance of the latter structural mode to the activation of CO for reduction,[6] we set out to prepare mixed Fe–Ru analogues of $[HFe_4(CO)_{13}]^-$ to determine if they too adopt this unusual bonding pattern and to assess the factors which influence this bonding mode. Herein we describe the preparation and spectroscopic and structural characterization of the $[HFe_2Ru_2(CO)_{13}]^-$ and $[HFeRu_3(CO)_{13}]^-$ anions as well as the first neutron diffraction structure determination of a member of the $[H_xM_4(CO)_{13}]^{(2-x)-}$ family. The geometries of $[HFe_2Ru_2(CO)_{13}]^-$ and $[HFeRu_3(CO)_{13}]^-$ have been found to be analogous to that of $H_2FeRu_3(CO)_{13}$ and $H_2Ru_4(CO)_{13}$ but not similar to that of $[HFe_4(CO)_{13}]^-$. These results further confirm prior suggestions[2,3] that the general location of the hydride ligand in the two neutral clusters is along the elongated Ru–Ru bond.

Experimental Section

$Ru_3(CO)_{12}$,[7] $FeRu_2(CO)_{12}$,[8] $Fe_2Ru(CO)_{12}$,[8] and $[(Ph_3P)_2N][HFe(CO)_4]$[9] were prepared according to published procedures. Tetrahydrofuran (THF) and Et_2O were dried by stirring over Na-benzophenone ketyl under N_2. Hexane was dried by stirring over CaH_2 under N_2. All other solvents employed were reagent grade. All solvents were deoxygenated, and all manipulations of compounds were conducted under a prepurified N_2 atmosphere unless otherwise specified.

Preparation of $[(Ph_3P)_2N][HFeRu_3(CO)_{13}]$. $Ru_3(CO)_{12}$ (0.297 g, 0.465 mmol) and $[(Ph_3P)_2N][HFe(CO)_4]$ (0.306 g, 0.433 mmol) were dissolved in 100 mL of dried THF and refluxed under an N_2 atmosphere for 4 h during which time the color of the solution changed from orange to brown. The THF was removed under vacuum and the residue dissolved in 20 mL of Et_2O. This solution was filtered and carefully layered with 20 mL of hexane at 0 °C. The layers were allowed to diffuse together overnight to yield black crystals of $[(Ph_3P)_2N][HFeRu_3(CO)_{13}]$ (0.259 g, 0.205 mmol, 47.4% yield): IR (THF) 2071 w, 2031 s, 2012 s, 1995 vs, 1964 m sh, 1940 m sh, 1850 w, 1824 m cm^{-1}. Anal. Calcd for $[(Ph_3P)_2N][HFeRu_3(CO)_{13}]$: C, 46.60; H, 2.48. Found: C, 45.94; H, 2.57 (Schwartzkopf Microanalytical Laboratory).

Preparation of $[(Ph_3P)_2N][HFe_2Ru_2(CO)_{13}]$. $Fe_2Ru(CO)_{12}$ (0.082 g, 0.149 mmol) and $[(Ph_3P)_2N][HFe(CO)_4]$ (0.109 g, 0.152 mmol) were dissolved in 24 mL of dried THF and refluxed under an N_2 atmosphere for 4 h during which time the color of the solution changed from deep purple to brown. The THF was removed under vacuum and the residue dissolved in 25 mL of Et_2O. This solution was filtered and carefully layered with 20 mL of hexane at 0 °C. The layers were allowed to diffuse together overnight to yield black crystals of $[(Ph_3P)_2N][HFe_2Ru_2(CO)_{13}]$ (0.007 g, 0.006 mmol, 4.0% yield): IR (THF) 2069 w, 2033 s, 2021 m, 1993 vs, 1930 m, 1820 m cm^{-1}. Anal. Calcd for $[(Ph_3P)_2N][HFe_2Ru_2(CO)_{13}]$: Fe, 9.17. Found: Fe, 8.99 (Alfred Bernhardt).

Crystallographic Summary

Pertinent crystal and intensity data for both compounds are listed in Table I. Relevant details for each compound are given below.

$[(Ph_3P)_2N][HFeRu_3(CO)_{13}]$. X-ray diffraction data were collected on a Syntex $P2_1$ automated diffractometer at the University of Southern California. The structure was solved by heavy-atom methods: a Patterson map was used to locate the metal core and difference-Fourier syntheses were used to locate the other nonhydrogen atoms.

---

[1] (a) Brookhaven National Laboratory. (b) The Pennsylvania State University. (c) University of Southern California. (d) Permanent address: Centro del CNR per la Sintesi e la Struttura dei Composti dei Metalli di Transizione nei Bassi Stati di Ossidazione, Via G. Venezian 21, I-20133, Milano, Italy.

[2] Yawney, D. B. W.; Doedens, R. J. *Inorg. Chem.* **1972**, *11*, 838.

[3] Gilmore, C. J.; Woodward, P. *J. Chem. Soc. A* **1971**, 3453.

[4] (a) Doedens, R. J.; Dahl, L. F. *J. Am. Chem. Soc.* **1966**, *88*, 4847. (b) A different tautomer of $[Fe_4(CO)_{13}]^{2-}$ with no semibridging CO's was recently observed in an X-ray diffraction study of $[Fe(C_5H_5N)_6][Fe_4(CO)_{13}]$ (Knobler, C. B.; Buskirk, G. V.; Kaesz, H. D., *Abstr. Amer. Cryst. Assoc. Mtg.*, Calgary, Alberta, Canada, August 17–22, 1980.

[5] Manassero, M.; Sansoni, M.; Longoni, D. *J. Chem. Soc., Chem. Commun.* **1976**, 919.

[6] Whitmire, K.; Shriver, D. F. *J. Am. Chem. Soc.* **1980**, *102*, 1456.

[7] Eady, R. E.; Jackson, P. F.; Johnson, B. F. G.; Lewis, J.; Malatesta, M. C.; McPartlin, M.; Nelson, J. H *J. Chem. Soc., Dalton Trans.* **1980**, 383.

[8] Yawney, D. B. W.; Stone, F. G. A. *J. Chem. Soc. A* **1969**, 502.

[9] Darensbourg, M. Y.; Darensbourg, D. J.; Barros, H. L. C. *Inorg. Chem.* **1978**, *17*, 297.

0020-1669/81/1320-3823$01.25/0 © 1981 American Chemical Society

Table I. Crystal and Intensity Data for $[(Ph_3P)_2N][HFeRu_3(CO)_{13}]$ and $[(Ph_3P)_2N][HFe_2Ru_2(CO)_{13}]$

	$[(Ph_3P)_2N][HFeRu_3(CO)_{13}]$		$[(Ph_3P)_2N][HFe_2Ru_2(CO)_{13}]$
	X-ray diffraction	neutron diffraction	X-ray diffraction
		Crystal Parameters	
crystal system	triclinic	triclinic	triclinic
space group	$P\bar{1}$	$P\bar{1}$	$P\bar{1}$
a, Å	15.229 (4)	15.053 (2)	14.955 (12)
b, Å	9.212 (6)	9.073 (1)	18.144 (3)
c, Å	19.347 (10)	18.992 (3)	9.290 (2)
α, deg	105.40 (5)	104.75 (2)	101.54 (2)
β, deg	109.40 (3)	109.58 (2)	95.03 (4)
γ, deg	86.50 (4)	86.94 (2)	84.04 (3)
V, Å^3	2467 (2)	2361.8 (4)	2451 (3)
Z	2	2	2
calcd density, g/cm^3	1.708	1.776 g/cm^3	1.589
cryst dimens, mm	0.6 × 0.4 × 0.4	cylindrical: 2.1 mm d. × 4.3 mm length	0.13 × 0.24 × 0.50
temp	20 °C	15 K	22 °C
		Intensity Data	
radiation (λ, Å)	Mo Kα (0.710 73)	neutron (1.1614 (2)[a])	Mo Kα (0.710 73)
monochromator	graphite crystal	germanium (220) crystal	graphite crystal
data limits, deg	$0 \leqslant 2\theta \leqslant 45$	$0 \leqslant 2\theta \leqslant 106$[b]	$0 \leqslant 2\theta \leqslant 50.0$
unique data	6312	9854	8690
nonzero data	4855 ($I > 3\sigma(I)$)	8354	5886 ($I > 3\sigma(I)$)
no. of parameters	452	903	622

[a] Calibrated with reference to KBr: $a = 6.6000$ Å at 25 °C. [b] A complete hemisphere in reciprocal space was sampled out to $2\theta = 85°$. A preliminary refinement based on these data was used to predict the strongest reflections beyond $2\theta = 85°$, and approximately 500 additional reflections were measured in each of two shells: $85° \leqslant 2\theta \leqslant 98°$ and $98° \leqslant 2\theta \leqslant 06°$.

Full-matrix least-squares refinement minimizing $\sum w(F_o - k|F_c|)^2$, with anisotropic temperature factors for all atoms except for the phenyl carbon atoms which were refined isotropically, led to the final agreement factors $R(F) = 0.071$ and $R(wF) = 0.096$ for 4855 observations where

$$R(F) = \sum||F_o| - k|F_c||/\sum|F_o|$$

$$R(wF) = [\sum w(|F_o| - k|F_c|)^2/\sum wF_o^2]^{1/2}$$

For the neutron diffraction study, an approximately cylindrical crystal (2.1 mm diameter × 4.3 mm length) was mounted on an Al pin, the end of which was hollow in order to reduce the amount of metal in the neutron beam, and was oriented with the crystallographic c axis approximately parallel to the pin. The sample was sealed in an Al can under an He atmosphere and placed in a closed-cycle refrigerator[10] mounted on a four-circle diffractometer at the Brookhaven high-flux beam reactor.[11] The temperature during data collection was 15 ± 0.5 K.[12] Lorentz and empirical absorption corrections were applied to the raw data to convert I into F_o^2 values. The variance of $F_o^2 = I \sin 2\theta$ for each reflection was estimated with use of the expression $[\sigma^2(F_o^2) = \sigma^2(F_o^2, \text{count}) + AF_o^4 + B]$, where A (0.00018 with F_o^2 on an absolute scale in barn units) and B (0.28) were estimated from the discrepancies between symmetry-related reflections ($hk0$ and $\bar{h}\bar{k}0$).

The atomic coordinates of the nonhydrogen atoms from the X-ray determination were used as initial values for the neutron study. After a few least-squares cycles, all hydrogen positions were located from a difference-Fourier map. Positional and anisotropic temperature factors for all atoms and a type I isotropic extinction correction parameter[13] were varied by block-diagonal least-squares refinement minimizing $\sum w(F_o^2 - k^2F_c^2)^2$ where $w = 1/\sigma^2(F_o^2)$. The scale factor (k) and overall temperature and isotropic extinction parameters were put in one (3 × 3) block while parameters of each atom were put in individual (9 × 9) blocks. Refinement was continued until the largest shift in any parameter was less than 0.3σ. The most significant extinction correction value applied to F_c^2 was 0.97 for the reflection (004). Neutron scattering lengths[14] used are $b_{Ru} = 0.721$, $b_{Fe} = 0.954$, $b_O = 0.580$, $b_N = 0.921$,[15] $b_C = 0.665$, and $b_H = -0.374 \times 10^{-12}$ cm. The final agreement factors are $R(F^2) = 0.052$ and $R(wF^2) = 0.057$ where

$$R(F^2) = \sum|F_o^2 - k^2|F_c|^2|/F_o^2$$

$$R(wF^2) = [\sum w(F_o^2 - k^2|F_c|^2)^2/\sum wF_o^4]^{1/2}$$

$[(Ph_3P)_2N][HFe_2Ru_2(CO)_{13}]$. X-ray diffraction data were collected on an Enraf-Nonius CAD4 diffractometer at The Pennsylvania State University. All programs used in the structure solution and refinement are part of the Enraf-Nonius structure determination package.[16] The data were collected and treated the same as described earlier.[17] The structure was solved by the heavy-atom method, a Patterson map was used to locate the metal core, and the coordinates of the remaining 65 nonhydrogen atoms were located by successive least-squares refinements and difference-Fourier maps. Block-diagonal-matrix least-squares refinement of the cluster and $[(Ph_3P)_2N]^+$ portions of the molecule with anisotropic temperature factors for all 69 nonhydrogen atoms reduced $R(F)$ to 0.056 and $R(wF)$ to 0.042, where $w = F_o/A2$ if $F_o < A2$ and $w = A2/F_o$ if $F_o \geq A2$ and $A2 = 77$.

Results

Synthesis and Spectral Characterization of $[(Ph_3P)_2N][HFeRu_3(CO)_{13}]$ and $[(Ph_3P)_2N][HFe_2Ru_2(CO)_{13}]$. Earlier studies have shown that the addition of a carbonylmetalate to a closed metal carbonyl trimer is a useful method for the synthesis of tetranuclear clusters.[17,18] For example, the addition of $[Fe(CO)_4]^{2-}$ to $Ru_3(CO)_{12}$, followed by protonation with H_3PO_4, gives $H_2FeRu_3(CO)_{13}$ in good yield (eq 1).[17a]

$$[Fe(CO)_4]^{2-} + Ru_3(CO)_{12} \xrightarrow{\Delta} \xrightarrow{H^+} \underset{\sim 49\%}{H_2FeRu_3(CO)_{13}} \quad (1)$$

Likewise, the addition of $[(Ph_3P)_2N][Co(CO)_4]$ to $Ru_3(CO)_{12}$

---

(10) Air Products and Chemicals Inc., DISPLEX® Model CS-202.

(11) (a) Dimmler, D. G.; Greenlaw, N.; Kelley, M. A.; Potter, D. W.; Rankowitz, S.; Stubblefield, F. W. *IEEE Trans. Nucl. Sci.* **1976**, *NS-23*, 398. (b) R. K. McMullan, and in part, L. C. Andrews, T. F. Koetzle, F. Reidinger, R. Thomas, and G. J. B. Williams NEXDAS, neutron and X-ray data acquisition system, unpublished work, 1976.

(12) Temperature measurements were calibrated with reference to the magnetic phase transition of FeF_2 at $T_N = 78.38$ (1) K.

(13) Becker, P. J.; Coppens, P. *Acta Crystallogr., Sect. A* **1975**, *A31*, 417.

(14) Koester, L. In "Neutron Physics", Koester, L., Steyerl, A., Eds.; Springer-Verlag: Berlin, Heidelberg, New York, 1977; p 36.

(15) Takusagawa, F.; Koetzle, T. F. *Acta. Crystallogr., Sect. B* **1979**, *B35*, 2126.

(16) Enraf-Nonius, Delft, Holland, 1975, revised 1977.

(17) (a) Gladfelter, W. L.; Geoffroy, G. L. *J. Am. Chem. Soc.* **1977**, *99*, 7565. (b) Steinhardt, P. C.; Gladfelter, W. L.; Harley, A. D.; Fox, J. R.; Geoffroy, G. L. *Inorg. Chem.* **1980**, *19*, 332.

(18) Gladfelter, W. L.; Geoffroy, G. L. *Adv. Organomet. Chem.* **1980**, *18*, 207.

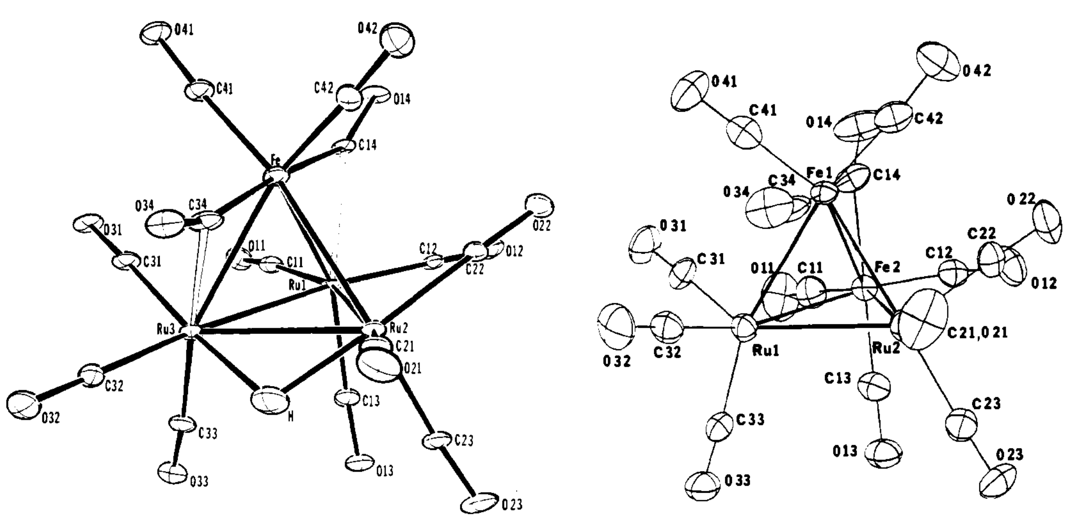

Figure 1. Comparison of the structures of $[HFeRu_3(CO)_{13}]^-$ (left, neutron diffraction, 97% probability ellipsoids) and $[HFe_2Ru_2(CO)_{13}]^-$ (right, X-ray diffraction, 25% probability ellipsoids).

allowed the isolation of $[(Ph_3P)_2N][CoRu_3(CO)_{13}]$ in nearly quantitative yield[17b] (eq 2). Following similar strategies, we

$$[(Ph_3P)_2N][Co(CO)_4] + Ru_3(CO)_{12} \xrightarrow{\Delta} \underset{95\%}{[(Ph_3P)_2N][CoRu_3(CO)_{13}]} \quad (2)$$

expected to isolate the desired $[HFe_xRu_{4-x}(CO)_{13}]^-$ anions by the reaction of $[HFe(CO)_4]^-$ with $Ru_3(CO)_{12}$, $FeRu_2(CO)_{12}$, and $Fe_2Ru(CO)_{12}$.

Indeed, heating $[(Ph_3P)_2N][HFe(CO)_4]$ with $Ru_3(CO)_{12}$ in refluxing THF for 1–3 h results in the isolation of $[(Ph_3P)_2N][HFeRu_3(CO)_{13}]$ as a dark brown crystalline solid in 47% yield (eq 3). However, the reaction of

$$[(Ph_3P)_2N][HFe(CO)_4] + Ru_3(CO)_{12} \xrightarrow{\Delta} \underset{47\%}{[(Ph_3P)_2N][HFeRu_3(CO)_{13}]} \quad (3)$$

$[(Ph_3P)_2N][HFe(CO)_4]$ with $FeRu_2(CO)_{12}$ did not yield the desired $[(Ph_3P)_2N][HFe_2Ru_2(CO)_{13}]$ product, but instead the only isolable product is a presently uncharacterized dark brown solid. The desired $[(Ph_3P)_2N][HFe_2Ru_2(CO)_{13}]$ compound was obtained in low yield from the reaction of $[(Ph_3P)_2N]$-$[HFe(CO)_4]$ with $Fe_2Ru(CO)_{12}$ (eq 4), a reaction which we

$$[(Ph_3P)_2N][HFe(CO)_4] + Fe_2Ru(CO)_{12} \xrightarrow[3\ h]{\Delta} \underset{4\%}{[(Ph_3P)_2N][HFe_2Ru_2(CO)_{13}]} \quad (4)$$

expected to produce the $[HFe_3Ru(CO)_{13}]^-$ anion. All attempts to prepare $[(Ph_3P)_2N][HFe_3Ru(CO)_{13}]$ have thus far failed. The failure of the reactions employing $FeRu_2(CO)_{12}$ and $Fe_2Ru(CO)_{12}$ to proceed as expected is likely due to the apparent relative ease with which these trimers fragment under the reaction conditions.[17]

The $[(Ph_3P)_2N][HFeRu_3(CO)_{13}]$ and $[(Ph_3P)_2N]$-$[HFe_2Ru_2(CO)_{13}]$ compounds have been fully characterized by elemental analysis, IR and ^1H NMR spectra, and complete single-crystal structure determinations. The IR spectra of both compounds show bands in the terminal and bridging regions (see Experimental Section), but none that might be indicative of a σ–π sideways-bound CO were observed. The ^1H NMR spectrum of $[HFe_2Ru_2(CO)_{13}]^-$ shows a temperature-invariant singlet in acetone-d_6 at δ −14.6 indicative of a metal-bound hydrogen. However, the ^1H NMR spectrum of $[HFeRu_3(CO)_{13}]^-$ shows two temperature-invariant singlets at δ −15.5 and −15.7 in acetone-d_6 in a ~6/1 ratio. The δ −15.7 singlet is similar to that reported for $[(Ph_3P)_2N][HRu_4(CO)_{13}]$ by Shore and co-workers[19] and may indicate that the samples of $[(Ph_3P)_2N][HFeRu_3(CO)_{13}]$ studied by ^1H NMR contain a small amount of the tetraruthenium cluster. The presence of such an impurity is not unreasonable in view of the fragmentation tendencies noted above and in ref 17 and is consistent with the elemental analysis of the compound which is low in carbon. Alternatively, the ^1H NMR signals could imply the presence of two different structural isomers of $[HFeRu_3(CO)_{13}]^-$, although it is difficult to imagine why the two isomers would not readily interconvert and give an averaged resonance as the temperature is raised.

Description of the Structures of $[(Ph_3P)_2N][HFeRu_3(CO)_{13}]$ and $[(Ph_3P)_2N][HFe_2Ru_2(CO)_{13}]$. The final atomic positional and thermal parameters of $[(Ph_3P)_2N][HFeRu_3(CO)_{13}]$ and $[(Ph_3P)_2N][HFe_2Ru_2(CO)_{13}]$ are respectively listed in Tables A, B, E, and F of the supplementary material. Selected bond distances and angles for the two clusters are given in Tables II–V. The labeling scheme used for $[HFeRu_3(CO)_{13}]^-$ corresponds to that published for $H_2FeRu_3(CO)_{13}$.[3] The labeling scheme employed for $[HFe_2Ru_2(CO)_{13}]^-$ is similar but with Fe(2) substituted for Ru(1); Ru(1) in $[HFe_2Ru_2(CO)_{13}]^-$ is analogous to Ru(3) in $[HFeRu_3(CO)_{13}]^-$. Listings of the final observed and calculated structure factors for the X-ray and neutron analyses are available in Tables C, D, and G in the supplementary material. The structures are shown in comparative views in Figures 1–3.

Both anions have distorted tetrahedral cores. For $[HFeRu_3(CO)_{13}]^-$, the metal–metal bond distances are similar to those reported for $H_2FeRu_3(CO)_{13}$[3] with the exception of the Ru(1)–Ru(2) edge which is deprotonated. This edge is found to be about 0.2 Å shorter in the absence of the hydride bridge. The Fe–Ru distances average 2.709 (1) Å, the unbridged Ru–Ru distances average 2.765 (2) Å, and the H^--bridged Ru–Ru distance is 2.916 (2) Å (neutron results). There are three terminal carbonyl groups on each Ru atom and four carbonyls attached to the Fe atom. Two of the carbonyls on the Fe atom are terminal, and the other two are asymmetrically bridging to Ru(1) and Ru(3). There is a slight tilting of the $Fe(CO)_4$ unit relative to the Ru_3 basal plane, best illustrated by the drawings shown in Figure 2.

The metal–metal distances (Å) in $[HFe_2Ru_2(CO)_{13}]^-$ are as follows: Fe–Fe, 2.624 (1); Fe–Ru_{av}, 2.675 (1); Ru–Ru, 2.892 (1). The length of the Ru–Ru vector is consistent with the hydride bridging this bond. Each of the four metal atoms bears three terminal carbonyls with an additional carbonyl bridging the Fe–Fe bond in a symmetrical fashion. With

---

[19] Nagel, C. C.; Shore, S. C. *J. Chem. Soc., Chem. Commun.* **1980**, 530.

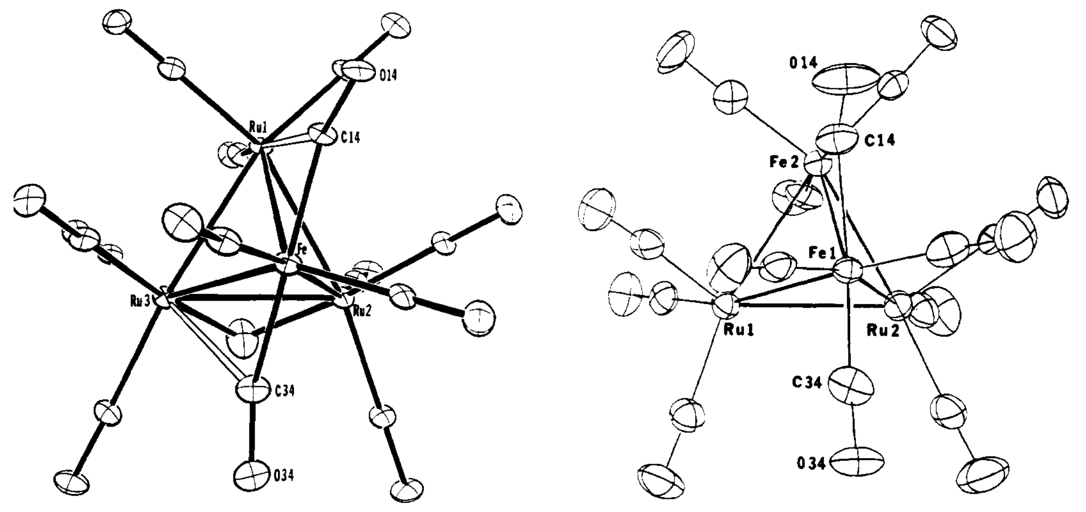

Figure 2. Comparative view of the structures of $[HFeRu_3(CO)_{13}]^-$ (left, neutron diffraction, 97% probability ellipsoids) and $[HFe_2Ru_2(CO)_{13}]^-$ (right, X-ray diffraction, 25% probability ellipsoids) that shows the relative orientations of the $Fe(CO)_4$ groups.

Table II. Selected Bond Distances (Å) in $[(Ph_3P)_2N][HFeRu_3(CO)_{13}]$

	neutron	X-ray
(a) Metal-Metal Distances		
Fe-Ru(1)	2.726 (2)	2.752 (2)
Fe-Ru(2)	2.724 (2)	2.708 (2)
Fe-Ru(3)	2.678 (2)	2.682 (2)
Ru(1)-Ru(2)	2.734 (2)	2.725 (2)
Ru(1)-Ru(3)	2.796 (2)	2.769 (1)
Ru(2)-Ru(3)	2.916 (2)	2.902 (1)
(b) Metal-Carbon Distances		
Fe-C(14)	1.915 (2)	1.89 (1)
Fe-C(34)	1.850 (2)	1.75 (2)
Fe-C(41)	1.813 (2)	1.78 (1)
Fe-C(42)	1.809 (2)	1.70 (2)
Ru(1)-C(11)	1.925 (2)	1.93 (1)
Ru(1)-C(12)	1.894 (2)	1.86 (1)
Ru(1)-C(13)	1.890 (2)	1.86 (1)
Ru(2)-C(21)	1.914 (2)	1.88 (1)
Ru(2)-C(22)	1.887 (2)	1.87 (2)
Ru(2)-C(23)	1.897 (2)	1.88 (2)
Ru(3)-C(31)	1.894 (2)	1.88 (1)
Ru(3)-C(32)	1.928 (2)	1.89 (1)
Ru(3)-C(33)	1.889 (2)	1.83 (1)
(c) Metal-Carbon Semibridging Distances		
Ru(1)-C(14)	2.241 (2)	2.23 (2)
Ru(3)-C(34)	2.438 (2)	2.54 (2)
(d) Carbon-Oxygen Distances		
C(11)-O(11)	1.151 (2)	1.09 (2)
C(12)-O(12)	1.146 (2)	1.14 (2)
C(13)-O(13)	1.149 (2)	1.11 (2)
C(14)-O(14)	1.170 (2)	1.20 (2)
C(21)-O(21)	1.157 (2)	1.13 (2)
C(22)-O(22)	1.154 (2)	1.13 (2)
C(23)-O(23)	1.148 (3)	1.17 (2)
C(31)-O(31)	1.167 (2)	1.16 (2)
C(32)-O(32)	1.152 (2)	1.10 (2)
C(33)-O(33)	1.137 (2)	1.17 (2)
C(34)-O(34)	1.170 (2)	1.21 (2)
C(41)-O(41)	1.158 (3)	1.17 (2)
C(42)-O(42)	1.138 (2)	1.20 (2)
(e) Metal-Hydrogen Distances		
Ru(2)-H	1.824 (3)	
Ru(3)-H	1.818 (4)	

$[HFe_2Ru_2(CO)_{13}]^-$, the tilting of the $Fe(CO)_4$ unit is even more pronounced relative to $[HFeRu_3(CO)_{13}]^-$ (Figure 2).

The H atom in $[HFeRu_3(CO)_{13}]^-$ is, as expected, bridging the long Ru(2)-Ru(3) edge [2.916 (2) Å] of the cluster. It is situated in an essentially symmetrical position, as the two Ru-H distances [Ru(2)-H = 1.818 (4) Å, Ru(3)-H = 1.824 (3) Å] agree within 2σ. The average Ru-H distance of 1.821 (3) Å found here compares well with other values derived from single-crystal neutron diffraction work: 1.792 (5) Å in $HRu_3(CO)_9(-C{\equiv}C\text{-}t\text{-}Bu)$[20] and 1.773 (2) Å in $H_4Ru_4(CO)_8[P(OMe)_3]_4$.[21] Other Ru-H (bridging) values, derived from X-ray data, include 1.85 (4) from $HRu_3(CO)_{10}(CNMe_2)$,[22] 1.76 $(6)_{av}$ and 1.70 $(12)_{av}$ Å from two different isomers of $H_4Ru_4(CO)_{10}(Ph_2PCH_2CH_2PPh_2)$,[23] and 1.77 $(6)_{av}$ Å in $H_3CoRu_3(CO)_{12}$.[24] A full listing of Ru-H distances measured to date is given in a recent review article.[25] The Ru-H-Ru bond is found in a characteristically bent configuration [106.4 (2)°], again consistent with other neutron-derived values: 102.3 (2)° in $HRu_3(CO)_9(-C{\equiv}C\text{-}t\text{-}Bu)$[20] and 114.2 (3)° in $H_4Ru_4(CO)_8[P(OMe)_3]_4$.[21]

The H atom is not directly situated on a pseudo-mirror plane of the tetrahedron [i.e., the plane defined by Ru(2), Ru(3) and the midpoint of the Fe-Ru(1) bond] but is tilted slightly toward Ru(1) (Figure 3). Thus, the dihedral angle between the planes Ru(2)Ru(3)H and Ru(1)Ru(2)Ru(3) is 47.7°, while that between Ru(2)Ru(3)H and Ru(2)Ru(3)Fe is only 24.5°.

The tilting of the $Fe(CO)_4$ fragment relative to the Ru_3 plane is shown in Figure 2. This is best appreciated by examining the distances associated with the semibridging CO groups: in $[HFeRu_3(CO)_{13}]^-$, the Ru(1)-C(14) distance [2.241 (2) Å] is significantly shorter than the Ru(3)-C(34) distance [2.438 (2) Å], in contrast to the situation in $H_2FeRu_3(CO)_{13}$ in which these two weak Ru-C interactions are essentially equal. The tilting is even more severe in $[HFe_2Ru_2(CO)_{13}]^-$ in which the CO(14) is best described as a symmetrically bridging carbonyl with Fe-C distances of 1.932 (9) and 2.008 (9) Å to Fe(1) and Fe(2), respectively. The Ru(1)-C(34) distance is much larger [2.616 (9) Å] than that of $[HFeRu_3(CO)_{13}]^-$, and CO(34) is best described as a normal terminal carbonyl with little or no semibridging characteristics. This tilting may reflect the distribution of negative charge in the clusters. It suggests a greater locali-

---

[20] Catti, M.; Gervasio, G.; Mason, S. S. *J. Chem. Soc., Dalton Trans.* **1977**, 2260.

[21] Orpen, A. G. Ph.D. Thesis, University of Cambridge, 1979.

[22] Churchill, M. R.; DeBoer, B. G.; Rotella, F. G. *Inorg. Chem.* **1976**, *15*, 1843.

[23] (a) Churchill, M. R.; Lashewycz, R. A. *Inorg. Chem.* **1978**, *17*, 1950. (b) Churchill, M. R.; Lashewycz, R. A.; Shapley, J. R.; Richter, S. I. *Ibid.* **1980**, *19*, 1277.

[24] Gladfelter, W. L.; Geoffroy, G. L.; Calabrese, J. C. *Inorg. Chem.* **1980**, *19*, 2569.

[25] Teller, R. G.; Bau, R. *Struct. Bonding (Berlin)*, in press.

Table III. Selected Bond Angles (Deg) in $[(Ph_3P)_2N][HFeRu_3(CO)_{13}]$

	neutron	X-ray
(a) Metal–Metal–Metal Angles		
Ru(1)–Fe–Ru(2)	60.21 (4)	59.88 (4)
Ru(1)–Fe–Ru(3)	62.29 (4)	61.27 (4)
Ru(2)–Fe–Ru(3)	65.34 (5)	65.14 (5)
Ru(2)–Ru(1)–Fe	59.85 (5)	59.26 (4)
Ru(3)–Ru(1)–Fe	58.01 (4)	58.12 (4)
Ru(3)–Ru(1)–Ru(2)	63.65 (5)	67.75 (4)
Ru(1)–Ru(2)–Fe	59.94 (5)	60.87 (4)
Ru(3)–Ru(2)–Fe	56.57 (5)	57.00 (4)
Ru(3)–Ru(2)–Ru(1)	59.20 (5)	58.87 (3)
Ru(1)–Ru(3)–Fe	59.70 (4)	60.61 (4)
Ru(2)–Ru(3)–Fe	58.09 (5)	57.86 (4)
Ru(2)–Ru(3)–Ru(1)	57.14 (5)	57.38 (4)
(b) Carbon–Metal–Carbon Angles		
C(14)–Fe–C(34)	173.91 (9)	176.0 (6)
C(14)–Fe–C(41)	87.58 (8)	88.0 (6)
C(14)–Fe–C(42)	88.99 (7)	86.9 (7)
C(34)–Fe–C(41)	97.54 (8)	94.7 (7)
C(34)–Fe–C(42)	93.60 (7)	95.7 (7)
C(41)–Fe–C(42)	97.21 (8)	98.1 (7)
C(11)–Ru(1)–C(12)	99.78 (8)	95.7 (6)
C(11)–Ru(1)–C(13)	96.16 (8)	95.6 (6)
C(12)–Ru(1)–C(13)	90.36 (8)	91.0 (6)
C(14)–Ru(1)–C(11)	93.62 (8)	93.4 (5)
C(14)–Ru(1)–C(12)	79.54 (7)	82.6 (6)
C(14)–Ru(1)–C(13)	167.0 (1)	169.4 (5)
C(21)–Ru(2)–C(22)	98.30 (8)	96.8 (7)
C(21)–Ru(2)–C(23)	95.02 (9)	95.6 (6)
C(23)–Ru(2)–C(22)	95.18 (9)	94.7 (7)
C(31)–Ru(3)–C(33)	91.53 (8)	93.6 (6)
C(32)–Ru(3)–C(31)	97.87 (9)	97.5 (6)
C(32)–Ru(3)–C(33)	94.52 (8)	94.5 (6)
C(34)–Ru(3)–C(31)	98.72 (8)	100.7 (5)
C(34)–Ru(3)–C(32)	78.16 (6)	75.8 (5)
C(34)–Ru(3)–C(33)	168.10 (9)	163.5 (6)
(c) Metal–Metal–Hydrogen Angles		
Fe–Ru(2)–H	90.7 (1)	
Ru(1)–Ru(2)–H	86.3 (1)	
Ru(3)–Ru(2)–H	36.7 (1)	
Fe–Ru(3)–H	92.3 (1)	
Ru(1)–Ru(3)–H	84.6 (1)	
Ru(2)–Ru(3)–H	36.9 (1)	
(d) Metal–Carbon–Oxygen Angles		
Fe–C(14)–O(14)	146.7 (1)	147.2 (11)
Fe–C(34)–O(34)	157.8 (1)	160.1 (13)
Fe–C(41)–O(41)	176.0 (1)	172.3 (14)
Fe–C(42)–O(42)	177.4 (2)	175.4 (15)
Ru(1)–C(11)–O(11)	175.6 (1)	178.8 (13)
Ru(1)–C(12)–O(12)	179.6 (1)	176.0 (14)
Ru(1)–C(13)–O(13)	175.6 (1)	174.4 (12)
Ru(1)–C(14)–O(14)	131.7 (1)	129.3 (10)
Ru(2)–C(21)–O(21)	177.0 (2)	176.5 (15)
Ru(2)–C(22)–O(22)	178.3 (2)	177.1 (13)
Ru(2)–C(23)–O(23)	175.8 (1)	173.6 (13)
Ru(3)–C(31)–O(31)	177.1 (1)	177.7 (12)
Ru(3)–C(32)–O(32)	178.3 (2)	177.1 (12)
Ru(3)–C(33)–O(33)	175.3 (2)	174.3 (12)
Ru(3)–C(34)–O(34)	126.2 (1)	125.0 (11)
(e) (Metal–Bridge Carbon)–Metal Angles		
Ru(1)–C(14)–Fe	81.58 (6)	83.5 (5)
Ru(3)–C(34)–Fe	75.93 (6)	74.9 (5)
(f) Metal–Hydrogen–Metal Angle		
Ru(2)–H–Ru(3)	106.4 (2)	
(g) Carbon–Metal–Hydrogen Angles		
C(21)–Ru(2)–H	87.1 (1)	
C(22)–Ru(2)–H	173.9 (2)	
C(23)–Ru(2)–H	87.1 (1)	
C(31)–Ru(3)–H	173.9 (1)	
C(32)–Ru(3)–H	88.1 (1)	
(h) Metal–Metal–Carbon Angles		
Fe–Ru(1)–C(11)	109.56 (8)	111.9 (4)
Fe–Ru(1)–C(12)	115.85 (6)	117.7 (5)
Fe–Ru(1)–C(13)	138.19 (7)	136.4 (4)
Fe–Ru(1)–C(14)	44.01 (4)	43.0 (3)
Fe–Ru(2)–C(21)	105.25 (7)	104.3 (5)
Fe–Ru(2)–C(22)	85.22 (7)	87.4 (5)
Fe–Ru(2)–C(23)	159.47 (7)	159.6 (4)
Fe–Ru(3)–C(31)	83.71 (7)	85.6 (4)
Fe–Ru(3)–C(32)	119.07 (6)	113.4 (4)
Fe–Ru(3)–C(33)	146.40 (7)	152.0 (4)
Fe–Ru(3)–C(34)	42.08 (4)	39.1 (3)
Ru(1)–Fe–C(14)	54.41 (5)	53.5 (4)
Ru(1)–Fe–C(34)	119.90 (6)	122.5 (5)
Ru(1)–Fe–C(41)	116.88 (7)	116.1 (5)
Ru(1)–Fe–C(42)	125.63 (7)	123.5 (5)
Ru(1)–Ru(2)–C(21)	163.67 (9)	164.2 (5)
Ru(1)–Ru(2)–C(22)	87.76 (7)	88.3 (4)
Ru(1)–Ru(2)–C(23)	99.54 (7)	98.9 (4)
Ru(1)–Ru(3)–C(31)	89.43 (7)	88.6 (4)
Ru(1)–Ru(3)–C(32)	172.46 (9)	171.2 (4)
Ru(1)–Ru(3)–C(33)	87.10 (6)	91.4 (4)
Ru(1)–Ru(3)–C(34)	98.98 (6)	97.0 (3)
Ru(2)–Fe–C(14)	96.89 (7)	98.1 (4)
Ru(2)–Fe–C(34)	77.56 (7)	78.8 (5)
Ru(2)–Fe–C(41)	170.30 (7)	166.4 (5)
Ru(2)–Fe–C(42)	91.49 (7)	94.4 (6)
Ru(2)–Ru(1)–C(11)	159.28 (8)	160.5 (4)
Ru(2)–Ru(1)–C(12)	100.90 (8)	103.8 (5)
Ru(2)–Ru(1)–C(13)	84.62 (8)	83.5 (4)
Ru(2)–Ru(1)–C(14)	89.26 (6)	89.8 (3)
Ru(2)–Ru(3)–C(31)	137.69 (7)	138.3 (4)
Ru(2)–Ru(3)–C(32)	115.51 (8)	114.3 (4)
Ru(2)–Ru(3)–C(33)	109.88 (8)	109.2 (4)
Ru(2)–Ru(3)–C(34)	66.03 (5)	64.6 (4)
Ru(3)–Fe–C(14)	113.56 (6)	110.5 (4)
Ru(3)–Fe–C(34)	62.00 (5)	66.0 (5)
Ru(3)–Fe–C(41)	104.98 (7)	101.4 (5)
Ru(3)–Fe–C(42)	148.59 (8)	154.1 (6)
Ru(3)–Ru(1)–C(11)	95.66 (7)	96.8 (4)
Ru(3)–Ru(1)–C(12)	164.55 (9)	167.5 (5)
Ru(3)–Ru(1)–C(13)	87.91 (7)	86.5 (4)
Ru(3)–Ru(1)–C(14)	99.64 (6)	97.9 (3)
Ru(3)–Ru(2)–C(21)	107.86 (7)	109.5 (5)
Ru(3)–Ru(2)–C(22)	137.81 (9)	139.4 (4)
Ru(3)–Ru(2)–C(23)	114.30 (7)	112.2 (4)

zation of negative charge on Ru(1) of $[HFeRu_3(CO)_{13}]^-$, causing it to back-bond its excessive charge[26] onto the semibridging carbonyl group CO(14). Distortion of the tetrahedron is also observed in the Fe–Ru(3) bond distance [2.678 (2) Å] of $[HFeRu_3(CO)_{13}]^-$ which is shorter than the other two Fe–Ru bonds [2.726 (2), 2.724 (2) Å].

It is curious that, in the few situations in which H atoms bridge edges of a mixed-metal cluster, the hydride ligands prefer to coordinate to the heavier metals. In our NMR studies[27] of mixed Fe/Ru/Os clusters, for example, we found an exclusive preference of H for Ru–Ru, Ru–Os, and Os–Os edges and no evidence of H bridging an Fe–Fe, Fe–Ru, or Fe–Os edge. This phenomenon supports the notion that metal hydride complexes involving second- and third-row transition metals are generally more stable than those involving first-row transition metals.[28]

Discussion

There are a number of general types of geometries found in $[H_xM_4(CO)_{13}]^{2-x}$ clusters: (1) the closed, pseudotetrahedral

---

[26] (a) Cotton, F. A.; Troup, J. M. *J. Am. Chem. Soc.* **1974**, *96*, 1233. (b) Cotton, F. A. *Prog. Inorg. Chem.* **1976**, *21*, 1.

[27] Geoffroy, G. L.; Gladfelter, W. L. *J. Am. Chem. Soc.* **1977**, *99*, 6775.

[28] Kaesz, H. D.; Saillant, R. B. *Chem. Rev.* **1972**, *72*, 231.

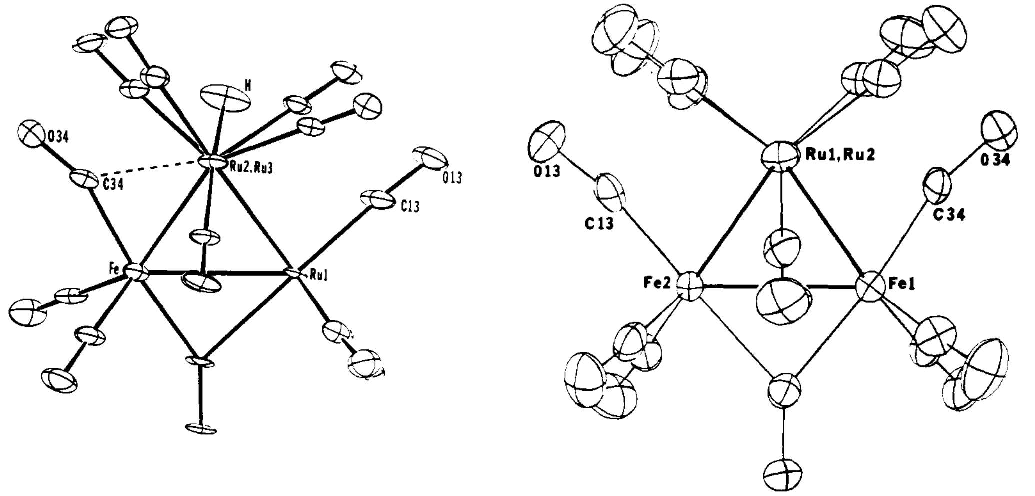

Figure 3. Comparative view of the structures of $[HFeRu_3(CO)_{13}]^-$ (left, neutron diffraction, 97% probability ellipsoids) and $[HFe_2Ru_2(CO)_{13}]^-$ (right, X-ray diffraction, 25% probability ellipsoids) that shows the relative positioning of the bridging carbonyls.

Table IV. Selected Bond Distances (Å) in $[(Ph_3P)_2N][HFe_2Ru_2(CO)_{13}]$

	(a) Metal-Metal Distances		
Ru(1)-Ru(2)	2.892 (1)	Ru(1)-Fe(1)	2.672 (1)
Ru(2)-Fe(1)	2.677 (1)	Ru(1)-Fe(2)	2.675 (1)
Ru(2)-Fe(2)	2.676 (1)	Fe(1)-Fe(2)	2.624 (1)
	(b) Metal-Carbon Distances		
Fe(2)-C(11)	1.749 (11)	Ru(1)-C(31)	1.867 (9)
Fe(2)-C(12)	1.750 (11)	Ru(1)-C(32)	1.903 (11)
Fe(2)-C(13)	1.759 (11)	Ru(1)-C(33)	1.880 (11)
Fe(1)-C(14)	1.932 (9)	Ru(1)-C(34)	1.616 (9)
Fe(2)-C(14)	2.008 (9)	Fe(1)-C(34)	1.721 (9)
Ru(2)-C(21)	1.870 (10)	Fe(1)-C(41)	1.763 (10)
Ru(2)-C(22)	1.892 (9)	Fe(1)-C(42)	1.765 (10)
Ru(2)-C(23)	1.898 (10)		
	(c) Carbon-Oxygen Distances		
C(11)-O(11)	1.180 (11)	C(31)-O(31)	1.160 (9)
C(12)-O(12)	1.190 (10)	C(32)-O(32)	1.119 (10)
C(13)-O(13)	1.162 (10)	C(33)-O(33)	1.142 (9)
C(14)-O(14)	1.178 (9)	C(34)-O(34)	1.183 (9)
C(21)-O(21)	1.143 (9)	C(41)-O(41)	1.162 (9)
C(22)-O(22)	1.113 (9)	C(42)-O(42)	1.149 (10)
C(23)-O(23)	1.137 (10)		

Table V. Selected Bond Angles (Deg) in $[(Ph_3P)_2N][HFe_2Ru_2(CO)_{13}]$

	(a) Metal-Metal-Metal Angles		
Fe(1)-Ru(2)-Fe(2)	58.7 (1)	Fe(2)-Fe(1)-Ru(2)	60.6 (1)
Fe(1)-Ru(2)-Ru(1)	57.2 (1)	Fe(2)-Fe(1)-Ru(1)	60.7 (1)
Fe(2)-Ru(2)-Ru(1)	57.3 (1)	Ru(2)-Fe(1)-Ru(1)	65.5 (1)
Fe(1)-Ru(1)-Fe(2)	58.8 (1)	Fe(1)-Fe(2)-Ru(2)	60.7 (1)
Fe(1)-Ru(1)-Ru(2)	57.4 (1)	Fe(1)-Fe(2)-Ru(1)	60.5 (1)
Fe(2)-Ru(1)-Ru(2)	57.3 (1)	Ru(2)-Fe(2)-Ru(1)	65.4 (1)
	(b) Metal-Carbon-Oxygen Angles		
Fe(2)-C(11)-O(11)	176.8 (10)	Ru(2)-C(23)-O(23)	176.6 (9)
Fe(2)-C(12)-O(12)	177.7 (8)	Ru(1)-C(31)-O(31)	177.0 (8)
Fe(2)-C(13)-O(13)	169.9 (9)	Ru(1)-C(32)-O(32)	176.8 (10)
Fe(1)-C(14)-O(14)	140.6 (8)	Ru(1)-C(33)-O(33)	176.3 (9)
Fe(2)-C(14)-O(14)	135.7 (8)	Fe(1)-C(34)-O(34)	164.6 (8)
Ru(2)-C(21)-O(21)	177.7 (8)	Fe(1)-C(41)-O(41)	177.4 (8)
Ru(2)-C(22)-O(22)	177.1 (8)	Fe(1)-C(42)-O(42)	176.8 (10)

cluster with 11 terminal and 2 semibridging carbonyls, as found in $H_2Ru_4(CO)_{13}$,[2] $H_2FeRu_3(CO)_{13}$,[3] and now observed with $[HFeRu_3(CO)_{13}]^-$; (2) the closed, pseudotetrahedral cluster with 12 terminal carbonyls and 1 bridging carbonyl as found with $[HFe_2Ru_2(CO)_{13}]^-$ and recently in $[HOs_4(CO)_{13}]^-$;[29] (3) the closed pseudotetrahedral cluster found in

Chart I

$[HRu_4(CO)_{13}]^-$	$[HFeRu_3(CO)_{13}]^-$	
presumably closed [in analogy with $H_2Ru_4(CO)_{13}$]	closed	
$[HFe_2Ru_2(CO)_{13}]^-$	$[HFe_3Ru(CO)_{13}]^-$	$[HFe_4(CO)_{13}]^-$
closed	?	open

$[Fe_4(CO)_{13}]^{2-}$,[4] with nine terminal and three semibridging carbonyls and one face-bridging carbonyl; (4) the "open-butterfly" arrangement found in $[HFe_4(CO)_{13}]^-$,[5,30] containing 12 terminal carbonyls and 1 highly unusual four-electron-donating carbonyl.

One way of rationalizing the open structure of $[HFe_4(CO)_{13}]^-$ with the closed structures of $[HFeRu_3(CO)_{13}]^-$ and $[HFe_2Ru_2(CO)_{13}]^-$ is to suggest that the closed Fe_4 tetrahedron is not large enough to accommodate 13 carbonyl groups and one hydride ligand on its surface, in contrast to the $FeRu_3$ and Fe_2Ru_2 clusters which are, as shown in this work, clearly large enough. It is interesting to speculate on where the cross-over point between the "closed" and "open" structures might be. The only member of the series whose structure is unknown is $[HFe_3Ru(CO)_{13}]^-$ (Chart I). Unfortunately, this anion and its neutral protonated analogue have so far defied all attempts at isolation.

Acknowledgment. This research was carried out under contract with the U.S. Department of Energy, Office of Basic Energy Sciences (G.L.G., T.F.K.), and supported by a National Science Foundation Grant CHE-77-00360 (to R.B.). We thank Mr. Joseph Henriques for technical assistance in operating the neutron diffractometer.

Registry No. $[(Ph_3P)_2N][HFeRu_3(CO)_{13}]$, 78571-90-1; $[(Ph_3P)_2N][HFe_2Ru_2(CO)_{13}]$, 78571-92-3; $[(Ph_3P)_2N][HFe(CO)_4]$, 56791-54-9; $Ru_3(CO)_{12}$, 15243-33-1; $Fe_2Ru(CO)_{12}$, 20468-34-2.

Supplementary Material Available: Listings of the final positional and thermal parameters and the structure factor amplitudes for the X-ray and neutron diffraction analyses (109 pages). Ordering information is given on any current masthead page.

---

(29) Dawson, P. A.; Johnson, B. F. G.; Lewis, J.; Kaner, D. A.; Raithby, P. R. *J. Chem. Soc., Chem. Commun.* **1980**, 961.

(30) The very recent discovery of the novel cluster species $HFe_4(\eta^2\text{-}CH)(CO)_{12}$ shows a geometry essentially identical with that of $[HFe_4(CO)_{13}]^-$. In this case, it is a C–H group which is bonding in a highly unusual fashion. The C atom is attached to all four Fe atoms while the C–H group is oriented in a "sideways" fashion to one of the iron atoms. $HFe_4(\eta^2\text{-}CH)(CO)_{12}$ and $[HFe_4(CO)_{13}]^-$ can be considered isoelectronic species, with the $\equiv$C—H group in one corresponding to the $\equiv$C—O$^-$ unit in the other. [Beno, M. A.; Williams, J. M.; Tachikawa, M.; Muetterties, E. L. *J. Am. Chem. Soc.* **1980**, *102*, 4542.]